Neurobiology of Aging 35 (2014) 1956.e1–1956.e8

Contents lists available at ScienceDirect

Neurobiology of Aging

journal homepage: www.elsevier.com/locate/neuaging

Genetic variation of oxidative phosphorylation genes in stroke and Alzheimer's disease

Alessandro Biffi [a,b,c,*], Mert R. Sabuncu [d,e], Rahul S. Desikan [f], Nick Schmansky [d], David H. Salat [a,g], Jonathan Rosand [a,b,c], Christopher D. Anderson [a,b,c], for the Alzheimer's disease Neuroimaging Initiative (ADNI)

[a] Division of Neurocritical Care and Emergency Neurology, Department of Neurology, Massachusetts General Hospital, Boston, MA, USA
[b] Center for Human Genetic Research, Massachusetts General Hospital, Boston, MA, USA
[c] Program in Medical and Population Genetics, Broad Institute, Cambridge, MA, USA
[d] Athinoula A. Martinos Center for Biomedical Imaging, Department of Radiology, Massachusetts General Hospital, Charlestown, MA, USA
[e] Computer Science and Artificial Intelligence Laboratory, Massachusetts Institute of Technology, Cambridge, MA, USA
[f] Department of Radiology, University of California, San Diego, CA, USA
[g] VA Boston Healthcare System, Boston, MA, USA

ARTICLE INFO

Article history:
Received 15 January 2014
Accepted 30 January 2014
Available online 5 February 2014

Keywords:
OXPHOS
Alzheimer's disease
Stroke
Mitochondria
Genes

ABSTRACT

Previous research implicates alterations in oxidative phosphorylation (OXPHOS) in the development of Alzheimer's disease (AD). We sought to test whether genetic variants within OXPHOS genes increase the risk of AD. We first used gene-set enrichment analysis to identify associations, and then applied a previously replicated stroke genetic risk score to determine if OXPHOS genetic overlap exists between stroke and AD. Gene-set enrichment analysis identified associations between variation in OXPHOS genes and AD versus control status ($p = 0.012$). Conversion from cognitively normal controls to mild cognitive impairment was also associated with the OXPHOS gene-set ($p = 0.045$). Subset analyses demonstrated association for complex I genes ($p < 0.05$), but not for complexes II–V. Among neuroimaging measures, hippocampal volume and entorhinal cortex thickness were associated with OXPHOS genes (all $p < 0.025$). The stroke genetic risk score demonstrated association with clinical status, baseline and longitudinal imaging measures ($p < 0.05$). OXPHOS genetic variation influences clinical status and neuroimaging intermediates of AD. OXPHOS genetic variants associated with stroke are also linked to AD progression. Further studies are needed to explore functional consequences of these OXPHOS variants.

1. Introduction

Late-onset Alzheimer's disease (AD) represents the most prevalent cause of dementia among Americans older than 65 years (Banerjee, 2012; Sosa-Ortiz et al., 2012). Despite the central role played by AD in pathologic brain aging, the causative mechanisms accounting for disease onset and progression remain only partially understood. Additional biological pathways influencing pathogenesis and disease course must be discovered if novel therapeutic targets are to be identified and exploited for treatment purposes.

Current evidence supports the hypothesis that alterations in function of the oxidative phosphorylation system (OXPHOS) plays a role in the pathogenesis of AD (Horan et al., 2012; Morán et al., 2012; Schmitt et al., 2012). Specifically, multiple observations have connected the toxic effects of beta-amyloid plaques and tau neurofibrillary tangles on the OXPHOS system to decreased neuronal survival (Eckert et al., 2010; Rhein et al., 2009). We sought to test the hypothesis that variation in genes involved with OXPHOS are associated with neuronal survival in neurodegenerative processes, by looking for associations between these variants and AD risk in individuals enrolled in the Alzheimer's disease neuroimaging initiative (ADNI). Furthermore, because

Data used in the preparation of this article were obtained from the Alzheimer's disease Neuroimaging Initiative (ADNI) database (www.loni.ucla.edu/ADNI). As such, the investigators within the ADNI contributed to the design and implementation of ADNI and/or provided data but did not participate in analysis or writing of this report. ADNI investigators include (complete listing available at http://adni.loni.usc.edu/wp-content/uploads/how_to_apply/ADNI_Acknowledgement_List.pdf).

* Corresponding author at: Center for Human Genetic Research, Massachusetts General Hospital, 185 Cambridge Street, CPZN-6818, Boston, MA 02114, USA. Tel.: +1 617 726 4369; fax: +1 617 643 3293.
E-mail address: abiffi@partners.org (A. Biffi).

0197-4580/$ – see front matter © 2014 Elsevier Inc. All rights reserved.
http://dx.doi.org/10.1016/j.neurobiolaging.2014.01.141

brain magnetic resonance imaging (MRI) and cerebrospinal fluid (CSF) biomarkers are potent predictors of AD risk and progression, we searched for associations between OXPHOS genes and these traits as well (Desikan et al., 2009; Dubois et al., 2010; Shaw et al., 2009).

A genetic risk score summarizing the cumulative effect of OXPHOS variants was recently found to associate with the risk of ischemic and hemorrhagic stroke, specifically stroke subtypes secondary to small vessel pathology, suggesting a link between OXPHOS variation and cerebrovascular disease (Anderson et al., 2013). Because radiographic markers of cerebral small vessel disease have previously been implicated in AD pathology and clinical progression, we sought to clarify whether these OXPHOS genetic variants known to associate with stroke are also associated with clinical and radiographic markers of AD, supporting a shared role of OXPHOS genetic variation in these 2 conditions (Kalaria, 2002; Kalaria et al., 2012; Snowdon et al., 1997; Thal et al., 2003).

In testing these 2 hypotheses, we first used a gene-set enrichment analysis (GSEA) technique to assess the global impact of OXPHOS genetic variation on AD and related phenotypes. We then applied the previously developed and replicated stroke genetic risk score to those same neurodegenerative phenotypes. The goal of the first set of analyses was to determine whether common variants within OXPHOS genes contain a greater degree of association with AD than would be expected by chance. The goal of the second set of analyses was to clarify whether the protective or deleterious influence of individual OXPHOS genetic variants are concordant when comparing AD and small vessel stroke.

2. Methods

2.1. ADNI

Data were obtained from the ADNI database (adni.loni.ucla.edu). The ADNI was launched in 2003 by the National Institute on Aging, the National Institute of Biomedical Imaging and Bioengineering, the Food and Drug Administration, private pharmaceutical companies and nonprofit organizations. ADNI is the result of efforts of many co-investigators from a broad range of academic institutions and private corporations, and subjects have been recruited from over 50 sites across the U.S. and Canada.

2.2. Subjects

Participants were screened, enrolled, and followed prospectively according to the previously published ADNI study protocol (Petersen et al., 2010). Participants were selected from the ADNI database as previously described (Biffi et al., 2010a). Briefly, included subjects were classified at baseline as:

1. Cognitively normal controls (CNC) with clinical dementia rating (CDR) = 0.
2. Mild cognitive impairment (MCI) individuals with Mini Mental State Examination scores between 24 and 30, a verified subjective memory complaint, objective memory loss, a CDR of 0.5, absence of significant levels of impairment in other cognitive domains, essentially preserved activities of daily living, an absence of dementia at the time of baseline MRI scan, and classified as amnestic MCI subtype.
3. AD individuals who met criteria for probable disease (CDR 1).

2.3. Genotype data

Individual-level single-nucleotide polymorphism (SNP) genotype data in the ADNI database were downloaded and merged to create a single dataset as previously described (Biffi et al., 2010a). Mitochondrial DNA (mtDNA) variants were downloaded and analyzed separately from autosomal DNA (autoDNA) data. All genetic analyses were performed using PLINK v1.07. Quality control of genotype data were implemented as previously described, and differed for mtDNA and autoDNA (Biffi et al., 2010b). Population structure was separately assessed for mtDNA and autoDNA by performing principal component analysis using published criteria (Anderson et al., 2013; Biffi et al., 2010b).

2.4. MRI data

ADNI MRI scans were acquired at multiple sites, and processed according to previously published methods using the FreeSurfer v4.5.0 (http://surfer.nmr.mgh.harvard.edu) software package (Biffi et al., 2010a). Five neuroimaging measures were chosen for analysis on the basis of their established role in predicting AD risk and progression: hippocampal volume, amygdala volume, entorhinal cortex thickness, parahippocampal gyrus thickness, and temporal pole cortex thickness (Biffi et al., 2010a). Measurement values at baseline and longitudinal change slopes were analyzed for these 5 neuroimaging traits.

2.5. CSF data

Baseline CSF samples were obtained in the morning after an overnight fast from 416 ADNI subjects (AD = 102, MCI = 200, CNC = 114) at time of enrollment according to published methods (Shaw et al., 2009). Amyloid beta 1–42 (Aβ42) total microtubule-associated protein tau (tau) levels were measured in each of the 416 CSF ADNI baseline aliquots using the multiplex xMAP Luminex platform (Luminex Corp, Austin, TX, USA) with Innogenetics (INNO-BIA AlzBio3; Ghent, Belgium) immunoassay kit–based reagents.

2.6. SNP selection

Before the selection of SNPs within OXPHOS genes, autosomal imputation was performed using PLINK v1.07 after quality control filtering. Mitochondrial imputation was performed using a haplotype-based approach with reference datasets from GenBank and Mitokor, according to previously published methods (Anderson et al., 2013). Genes encoding proteins directly involved in the OXPHOS respiratory chain were selected based on the published criteria from a chemical dissection of mitochondrial function (Wagner et al., 2008), yielding a total of 95 genes in the autosomal genome and 13 genes in the mitochondrial genome (see Supplementary Table 1). SNPs falling within these genes ±100 kilobases and passing quality control filtering were extracted from the ADNI data set (see Supplementary Table 2). Sub-analyses were performed for genes grouped according to each OXPHOS respiratory complex, classified according to annotation in the Ensembl Genome Browser (http://www.ensembl.org), as described elsewhere (Anderson et al., 2013).

2.7. Gene-set enrichment analyses

Testing for cumulative OXPHOS pathway associations with AD clinical status and related endophenotypes was performed using the GSEA method, as implemented in the GenGen v.2010Apr29

software package (Subramanian et al., 2005; Wang et al., 2007). The GSEA method tests whether variants within a predefined biological pathway contain more associations with the chosen phenotype than would be expected by chance alone (testing against the null hypothesis derived from random sampling of an equal number of variants of similar minor allele frequencies chosen from genes not within the OXPHOS pathway). We therefore used it to screen the multiple possible associations between the OXPHOS pathways (and its sub-complexes) and clinical, imaging, and CSF phenotypes (Fig. 1). Using this technique, the significance threshold for our GSEA analyses was set at permutation-derived $p < 0.05$.

2.8. Stroke genetic risk score generation and testing

Combined effects of autosomal and mitochondrial OXPHOS SNPs on stroke risk were evaluated in a previously published study, using a score-based method (Anderson et al., 2013). Briefly, each OXPHOS SNP was tested for association with ischemic stroke risk in a prospectively enrolled case–control stroke study at Massachusetts General Hospital (MGH, Boston, MA, USA). OXPHOS SNPs were classified into risk variants (logistic regression odds ratio [OR] for stroke >1.0) or protective variants (OR for stroke <1.0) based on these analyses (see Supplementary Table 3).

For each ADNI individual, a risk score was generated by adding a value of 1 for each stroke risk variant possessed, and a value of −1 for each stroke protective variant. Positive values identified individuals with net increased stroke genetic risk, whereas negative values identified subjects with net decreased stroke genetic risk. The stroke risk score was used as the independent variable in: (1) an ordinal logistic regression model for clinical status (AD vs. MCI vs. CNC); (2) logistic regression models for CNC progression to MCI and MCI progression to AD; and (3) linear regression analyses for CSF and imaging measures. For all these analyses, reported effect sizes refer to a unitary increase in stroke score value, and thus reflect the average effect of a single risk variant.

Based on prior results indicating a specific role for complex I variants in ischemic stroke, we opted to generate a separate score limiting the selection of SNPs to this complex (Anderson et al., 2013). Genetic risk scores including only variants from each of the other 4 complexes returned no statistically significant association with any of the analyzed phenotypes (data not shown). Distribution of stroke genetic risk score values for ADNI individuals (stratified by clinical status) is presented in Fig. 2.

All analyses included the following covariates: age, sex, history of hypertension, history of stroke, *APOE* genotype (number of ε2 and ε4 copies), alcohol abuse (DSM-IV criteria), smoking status (ever smoker), and education level (based on the number of school years attended: <13, 13–16, or >16 years). Population stratification was adjusted for according to previously published methods (Anderson et al., 2013; Biffi et al., 2010a, 2010b).

Because Bonferroni correction was inappropriate owing to the nonindependence of tested phenotypes we used the Benjamini–Hochberg false discovery rate (FDR) method to control for multiple hypothesis testing. Statistical significance was defined for FDR-corrected $p < 0.05$ (Biffi et al., 2010b; Hochberg and Benjamini, 1990).

3. Results

3.1. Study participants

A total of 818 ADNI subjects had genotype data available for analysis. Of these, 78 were excluded based on quality control criteria for genotype and MRI data. This resulted in 740 subjects with baseline MRI data available for analysis (Table 1). Among these, 604 (82%) had at least 1 follow-up MRI scan. We extracted data for 135 mtDNA SNPs and 707 autoDNA SNPs after ADNI data underwent imputation (Fig. 1). All included SNPs passed relevant quality control filters.

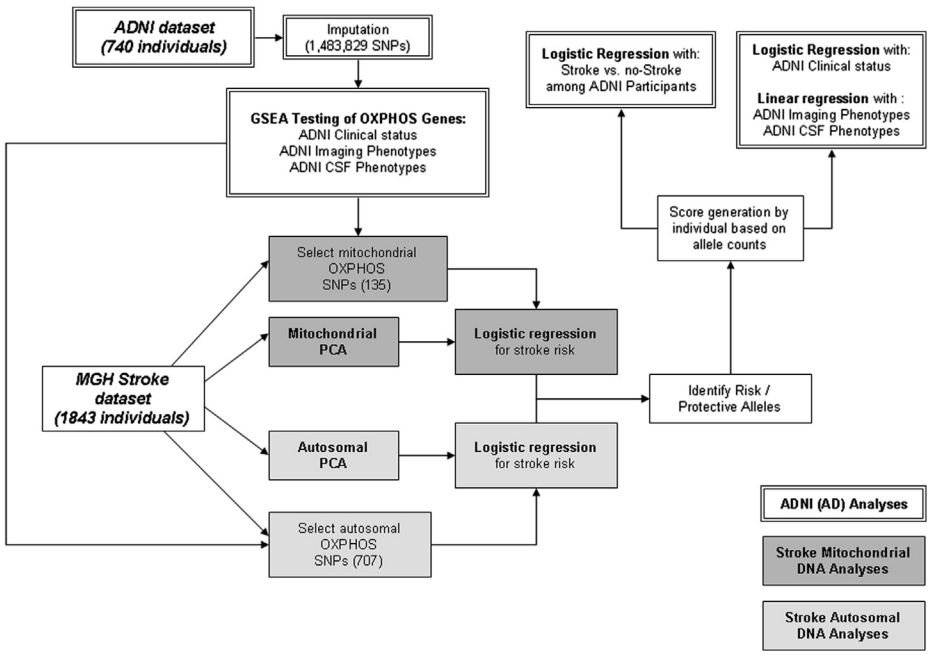

Fig. 1. Flow-chart of study design. Abbreviations: AD, Alzheimer's disease; ADNI, Alzheimer's disease neuroimaging initiative; CSF, cerebrospinal fluid; MGH, Massachusetts General Hospital; OXPHOS, oxidative phosphorylation; PCA, principal component analysis; SNP, single-nucleotide polymorphism.

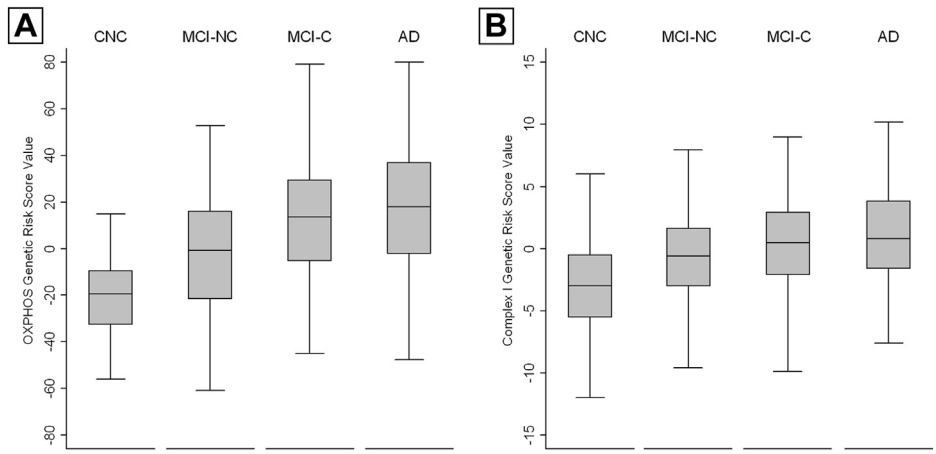

Fig. 2. OXPHOS genetic risk score individual values by clinical status among ADNI participants. (A) Genetic risk score individual values by clinical status, generated by incorporating variants from all OXPHOS genes. (B) Genetic risk score individual values by clinical status, generated by incorporating variants from complex I genes only. Abbreviations: AD, Alzheimer's disease; CNC, cognitively normal control; MCI-C, mild cognitive impairment subjects that converted to Alzheimer's disease diagnosis at follow-up; MCI-NC, mild cognitive impairment subjects that did not convert to Alzheimer's disease diagnosis at follow-up.

3.2. Gene-set enrichment analyses

The GSEA method was used to identify associations between the OXPHOS gene set and AD phenotypes. We identified association between OXPHOS genes and AD versus CNC status ($p = 0.012$), as well as with disease progression from CNC to MCI ($p = 0.045$). No association was identified for MCI conversion to AD. Subset analyses identified significant associations with clinical status for complex I only (AD vs. CNC $p = 0.002$, CNC to MCI conversion $p = 0.017$), suggesting that complex I is primarily responsible for the association with the full OXPHOS gene set. Among neuroimaging phenotypes, only hippocampal volume and entorhinal cortex

Table 1
Characteristics of ADNI study participants

	All subjects	Cognitively normal controls	MCI non-converters	MCI converters	Alzheimer's disease
Number of subjects	740	215	217	140	168
Follow-up time (median, IQR in mo)	12 (6–24)	12 (6–24)	12 (6–24)	18 (6–24)	12 (6–24)
Age (mean, SD in y)	75.3 (6.9)	75.9 (5.5)	75.3 (7.4)	74.6 (6.8)	75.5 (7.7)
Sex (% male)	41	45	34	39	48
Education (median, IQR in y)	16 (14–18)	16 (14–18)	16 (13–18)	16 (14–18)	16 (12–17)
History of hypertension (%)	47	45	47	49	51
Smoking (%)	39	36	42	39	40
Alcohol abuse (%)	4.1	2.3	3.7	5.0	5.9
Previous history of stroke (%)	1.9	1.0	2.3	2.1	1.8
CSF Aβ1-42[a] (median, IQR in pg/mL)	150 (128–216)	221 (162–256)	151 (125–216)	139 (119–158)	135 (121–160)
Tau[a] (median, IQR in pg/mL)	86 (60–122.5)	64 (51–86)	80 (54–126)	98 (78–123)	112.5 (77–155.5)
Amygdala volume (mean, SD in cc)	1.25 (0.22)	1.38 (0.19)	1.28 (0.20)	1.16 (0.19)	1.11 (0.18)
Hippocampal volume (mean, SD in cc)	3.23 (0.59)	3.66 (0.50)	3.28 (0.52)	2.95 (0.48)	2.85 (0.49)
Parahippocampal gyrus cortical thickness (mean, SD in mm)	2.34 (0.32)	2.49 (0.28)	2.36 (0.33)	2.27 (0.27)	2.18 (0.32)
Entorhinal cortical thickness (mean, SD in mm)	3.09 (0.47)	3.40 (0.30)	3.16 (0.45)	2.93 (0.43)	2.73 (0.43)
Temporal pole cortical thickness (mean, SD in mm)	3.48 (0.13)	3.66 (0.26)	3.52 (0.32)	3.37 (0.36)	3.29 (0.39)
Amygdala volume slope[b] (median, IQR)	−0.12 (−0.40/0.15)	0.03 (−0.19/0.23)	−0.13 (−0.37/0.12)	−0.23 (−0.48/0.07)	−0.30 (−0.58/0.03)
Hippocampal volume slope[b] (median, IQR)	−0.24 (−0.46/−0.06)	−0.13 (−0.27/0.01)	−0.18 (−0.40/−0.04)	−0.37 (−0.55/−0.19)	−0.43 (−0.61/−0.25)
Parahippocampal gyrus cortical thickness slope[b] (median, IQR)	−0.14 (−0.40/0.11)	0.01 (−0.19/0.22)	−0.08 (−0.29/0.07)	−0.29 (−0.50/−0.01)	−0.31 (−0.58/0.01)
Entorhinal cortical thickness slope[b] (median, IQR)	−0.21 (−0.47/0.03)	−0.07 (−0.24/0.13)	−0.16 (−0.36/0.05)	−0.42 (−0.68/−0.20)	−0.39 (−0.68/−0.16)
Temporal pole cortical thickness slope[b] (median, IQR)	−0.16 (−0.41/0.01)	−0.06 (−0.21/0.07)	−0.11 (−0.32/0.03)	−0.30 (−0.55/−0.04)	−0.33 (−0.64/−0.13)
APOE ε2 (MAF)	0.042	0.070	0.039	0.021	0.027
APOE ε4 (MAF)	0.367	0.142	0.290	0.432	0.430

Key: ADNI, Alzheimer's disease neuroimaging initiative; CSF, cerebrospinal fluid; IQR, inter-quartile range; MAF, minor allele frequency; MCI, mild cognitive impairment; MRI, magnetic resonance imaging; SD, standard deviation.

[a] CSF data obtained for 416 ADNI subjects (Alzheimer's disease = 102, MCI = 200, cognitively normal controls = 114).

[b] Results are expressed as a slope of change of MRI measures over time, with negative numbers indicating decrease in volume/thickness over time, and positive numbers indicating increase over time.

Table 2
GSEA association results for OXPHOS genes and imaging phenotypes

	All OXPHOS genes	Complex I	Complex II/III	Complex IV	Complex V
Baseline imaging measures					
Hippocampal volume	**0.006**	**2.0×10^{-4}**	—	*0.12*	—
Amygdala volume	—	—	—	*0.15*	—
Entorhinal cortex thickness	*0.14*	**0.043**	—	—	—
Parahippocampal gyrus thickness	—	—	—	—	
Temporal pole cortex thickness	—	*0.11*	—	—	—
Longitudinal change in imaging measures					
Hippocampal volume	**0.014**	**0.014**	—	—	—
Amygdala volume	—	—	—	—	—
Entorhinal cortex thickness	**0.021**	**0.008**	—	—	—
Parahippocampal gyrus thickness	*0.18*	—	—	—	
Temporal pole cortex thickness	—	—	—	—	—

This table reports *p*-values for GSEA association testing between gene sets and specific imaging phenotypes.
Values in bold identify results surpassing the pre-specified significance threshold of $p < 0.05$. Values in italics identify results with a non-significant trend toward association (p-values > 0.05 and < 0.20).
Key: GSEA, gene-set enrichment analysis; OXPHOS, oxidative phosphorylation.

thickness were associated with the OXPHOS gene set, both at baseline and longitudinally (Table 2). Subset analyses once again revealed an association between complex I and these same MRI measures. No associations were identified between OXPHOS genes and CSF biomarker data ($p > 0.20$).

3.3. Stroke genetic risk score replication in ADNI

Logistic regression analysis for the presence versus absence of prior stroke history showed an association with the OXPHOS genetic risk score (OR = 1.19, 95% confidence interval [95% CI] = 1.01–1.40, $p = 0.041$). Subset analyses revealed association between stroke history among ADNI subjects and the complex I stroke genetic risk score (OR = 1.23, 95% CI = 1.03–1.44, $p = 0.019$), but not with all other complexes (all $p > 0.20$). Based on these results, both the OXPHOS stroke genetic risk score and the complex I stroke genetic risk score were used in subsequent analyses.

3.4. Stroke genetic risk score extension to AD clinical status

We found an association between disease status (i.e., CNC–MCI–AD) and OXPHOS stroke genetic risk score (OR = 1.01, 95% CI = 1.01–1.02, FDR-$p = 0.048$). No associations were identified with the risk of conversion from CNC to MCI, or from MCI to AD. Based on the previously mentioned findings and from our prior OXPHOS stroke genetic association study (Anderson et al., 2013), we separately tested associations with the complex I stroke genetic risk score. We identified an association between disease status (CNC–MCI–AD) and complex I risk score (OR = 1.05, 95% CI = 1.01–1.10, FDR-$p = 0.049$), as well as with risk of CNC conversion to MCI (OR = 1.08, 95% CI = 1.01–1.15, FDR-$p = 0.04$), but not for the risk of MCI conversion to AD, matching the results obtained through GSEA.

3.5. Stroke genetic risk score extension to AD imaging measurements

Among neuroimaging phenotypes, only hippocampal volume was associated with the OXPHOS stroke genetic risk score at baseline (coefficient = −1.80, 95% CI = −3.03/−0.57, FDR-$p = 0.009$), but not longitudinally ($p > 0.20$). We identified a nonsignificant trend toward the association between the risk score and entorhinal cortex thickness at baseline ($p = 0.13$), but not longitudinally ($p > 0.20$).

We also identified the associations between the complex I stroke genetic risk score and hippocampal volume and entorhinal cortex thickness, again paralleling results obtained through GSEA (Table 3). Associations were identified for both traits at baseline, although longitudinal change in hippocampal volume was associated with the risk score. Analyses of association between other OXPHOS complexes and imaging measures returned no significant associations (data not shown).

The identification of a specific association between complex I risk score with CNC conversion to MCI (but not with MCI conversion to AD), as well as visual inspection of score values distribution plots by clinical status (Fig. 2), led us to hypothesize that

Table 3
Associations between complex I stroke genetic risk score and MRI neuroimaging measures

	Beta coeff.	95% CI	*p*	FDR-*p*
Baseline imaging measures				
Hippocampal volume[a]				
All subjects	−20.47	−34.18/−6.76	**0.003**	**0.004**
CNC (n = 205)	−34.8	−66.0/−3.0	**0.032**	**0.039**
MCI (n = 364)	−22.8	−45.3/−0.2	**0.045**	**0.048**
AD (n = 171)	−3.24	−28.1/21.7	—	—
Entorhinal cortex thickness				
All subjects	−0.003	−0.001/−0.005	**0.041**	**0.046**
CNC (n = 205)	−0.009	−0.001/−0.016	**0.022**	**0.030**
MCI (n = 364)	−0.0021	−0.011/0.075	—	—
AD (n = 171)	0.00	−0.004/0.004	—	—
Longitudinal change in imaging measures[b]				
Hippocampal volume				
All subjects	−0.007	−0.015/−0.001	**0.012**	**0.017**
CNC	−0.008	−0.016/−0.001	**0.018**	**0.021**
MCI	−0.006	−0.014/−0.001	**0.022**	**0.028**
AD	−0.001	−0.009/0.006	—	—
Entorhinal cortex thickness				
All subjects	−0.009	−0.028/0.021	*0.13*	*0.16*
CNC	−0.012	−0.029/0.053	*0.17*	*0.19*
MCI	−0.002	−0.003/−0.001	**0.033**	**0.039**
AD	0.001	−0.015/0.016	—	—

This table reports *p*-values for association testing between the complex I Genetic Risk Score and specific neuroimaging measures. Statistical significance identified by FDR $p < 0.05$.
Values in bold identify results surpassing the pre-specified significance threshold of $p < 0.05$. Values in italics identify results with a non-significant trend toward association (p-values > 0.05 and < 0.20).
Key: AD, Alzheimer's disease; CI, confidence interval; CNC, cognitively normal controls; Coeff, coefficient; FDR, false discovery rate; MCI, mild cognitive impairment; MRI, magnetic resonance imaging.
[a] Results are expressed in terms of mm^3 of volume for ease of interpretation.
[b] Results are expressed as a slope of change of MRI measures over time, with negative numbers indicating decrease in volume/thickness over time, and positive numbers indicating increase over time.

the effect of the genetic risk score on neuroimaging measurements might be specific to the earlier stages of disease progression in AD. We therefore opted to repeat association testing for the complex I risk score and imaging measures within strata identified by clinical status at baseline (Table 3). Indeed, associations between the complex I score and hippocampal volume were present only for CNC and MCI subjects. Entorhinal cortex was associated with complex I score at baseline only for CNC subjects, and as a longitudinal change only for MCI subjects (with nonsignificant trends toward association for CNC subjects and longitudinal change).

4. Discussion

Our analyses demonstrate associations between the cumulative effect of common OXPHOS DNA sequence variants and AD clinical spectrum, ranging from normal elderly controls to MCI subjects, to patients with a clinical diagnosis of AD. Several AD-related MRI imaging measures were also associated with OXPHOS gene variants. Furthermore, we have shown associations between a previously developed and independently replicated stroke genetic risk score and AD clinical status, as well as with the previously mentioned neuroimaging phenotypes.

Previously accumulated evidence has implicated the OXPHOS system in AD onset and progression (Eckert et al., 2010; Horan et al., 2012; Morán et al., 2012; Rhein et al., 2009; Schmitt et al., 2012; Verri et al., 2012). Our GSEA identified associations between SNPs within OXPHOS genes and clinical status, providing evidence that common variation within the 105 genes directly contributing structural proteins to the OXPHOS system is associated with the clinical manifestations leading from normal brain aging to AD. In support of this clinical association, 2 of the MRI imaging traits, most predictive of disease progression (hippocampal volume and entorhinal cortex thickness) were also associated with OXPHOS genetic variation. The lack of association between the OXPHOS gene-set and beta-amyloid and tau CSF levels (which are reflective of the overall brain burden for both protein products) provides suggestive evidence against a role for the mitochondrial respiratory machinery in determining the accumulation or clearance of these abnormal proteins (Shaw et al., 2009). Overall, our findings support the hypothesis that genetic variation within OXPHOS genes modulates the natural resilience of mitochondrial respiratory activity, thus, impacting the pace of degeneration of key cerebral structures in AD and, ultimately, disease progression.

Our GSEA identified associations between OXPHOS variants and hippocampal volume and entorhinal cortex thickness but not among the other disease-related imaging traits were tested. These findings can be interpreted in several ways. Based on the previously accumulated data, the hippocampus and entorhinal cortex appear to be particularly vulnerable to oxidative damage (Beal, 1995; Chen et al., 2010; de la Torre, 2008). However, it is entirely possible that the associations between OXPHOS genetic variation and these 2 phenotypes simply reflect their higher predictive power in determining AD onset and progression, as previously reported (Biffi et al., 2010a; Killiany et al., 2000). Finally, limited power in the ADNI dataset and the play of chance could explain a portion of the observed findings.

Our prior and present analyses have consistently shown a predominant role for complex I above other OXPHOS complexes (Anderson et al., 2013). These observations could be influenced by chance and/or by leveraging statistical power, given that complex I accounts for 50 of the 105 structural genes belonging to the OXPHOS pathway. Alternatively, complex I mutations account for up to one-third of the known respiratory chain diseases, and represent the main determinant of cellular redox state; this biological primacy could translate into a preeminent role in AD and stroke risk (Stefanatos and Sanz, 2011).

Our analyses demonstrate that an OXPHOS (specifically, complex I) genetic risk score, developed and replicated for prediction of stroke risk, was also significantly associated with AD clinical status and neuroimaging measures. These findings support the existence of overlap in genetic architecture between small vessel stroke and AD, suggest a shared role for OXPHOS in both conditions, and represent independent support for the findings obtained through GSEA. The analyses presented in this study suggest a preferential role for these OXPHOS variants in determining AD evolution in the earlier stages (i.e., conversion from CNC to MCI, as well as imaging traits in MCI subjects). A possible unifying hypothesis for these cross-disease associations rests on the putative role of the OXPHOS machinery in response to chronic neuronal insults, be they related to cerebrovascular risk factors or neurodegeneration.

Limitations render our results hypothesis-generating. Because of the unique extensive phenotyping of the ADNI cohort, our results cannot be readily replicated in an independent dataset. However, the multiple concordant findings are highly unlikely to be because of chance alone, and their validity is further supported by permutation testing (for GSEA), and by the development of the original stroke genetic risk score in an independent dataset comprised cases and controls for a different disease. More definitive conclusions with correspondingly greater study power will require independent replication and meta-analysis in larger datasets currently under development (Weiner et al., 2012). We are also unable, by nature of our analytical design, to identify specific genes or SNPs associated with the analyzed phenotypes. Additional efforts in functional dissection and annotation of OXPHOS genes will be required to identify the causative variants, likely through high-throughput sequencing, as is rapidly becoming an accepted standard in the field (Bettens et al., 2013).

In summary, we have identified associations between common genetic variation within OXPHOS genes and AD clinical status and neuroimaging correlates, with consistent results indicating a preeminent role for complex I genes. Furthermore, the cumulative genetic influence of OXPHOS genes on ischemic stroke translates into directly overlapping associations with AD and related MRI traits. Future studies will be required to confirm these findings, and expand our understanding of the role of the mitochondrial respiratory activity in chronic brain response to cerebrovascular and neurodegenerative processes. Ultimately, the elucidation of these mechanisms could lead to novel therapies for ischemic and neurodegenerative cognitive disorders of aging.

Disclosure statement

Mr Nick Schmansky has a financial interest in CorticoMetrics, a company whose medical pursuits focus on brain imaging and measurement technologies. His interests were reviewed and are managed by Massachusetts General Hospital and Partners HealthCare in accordance with their conflict of interest policies. No other conflicts of interest exist for any of the named authors in this study. The authors certify that all their affiliations with or financial involvement, within the past 5 years and foreseeable future (e.g., employment, consultancies, honoraria, speakers bureau, stock ownership or options, expert testimony, grants or patents received or pending, royalties, or donation of medical equipment) with any organization or entity with a financial interest in or financial conflict with the subject matter or materials discussed in the manuscript are completely disclosed. All authors had full access to all the data in the study and take

responsibility for the integrity of the data and the accuracy of the data analysis. There are no actual or potential conflicts of interest to disclose.

Acknowledgements

This work was supported by grants from the National Center for Research Resources (grant numbers P41-RR14075, R01 RR 16594-01A1); the NCRR BIRN Morphometric Project (grant numbers BIRN002, U24 RR021382); the National Institute for Biomedical Imaging and Bioengineering (grant number R01 EB001550); the Mental Illness and Neuroscience Discovery Institute; and the National Institute on Aging (grant numbers P50 AG05681, P01AG03991, and AG021910). Data collection and sharing for this project was funded by the Alzheimer's disease Neuroimaging Initiative (ADNI; Principal Investigator: Michael Weiner); National Institutes of Health grant number U01 AG024904 and the Howard Hughes Medical Institute (OASIS project). ADNI is funded by the National Institute on Aging; the National Institute of Biomedical Imaging and Bioengineering (NIBIB); and through generous contributions from the following: Pfizer Inc, Wyeth Research, Bristol-Myers Squibb, Eli Lilly and Company, GlaxoSmithKline, Merck & Co Inc, AstraZeneca AB, Novartis Pharmaceuticals Corporation, Alzheimer's Association, Eisai Global Clinical Development, Elan Corporation plc, Forest Laboratories, and the Institute for the Study of Aging, with participation from the U.S. Food and Drug Administration. Industry partnerships are coordinated through the Foundation for the National Institutes of Health. The grantee organization is the Northern California Institute for Research and Education, and the study is coordinated by the Alzheimer's disease Cooperative Study at the University of California, San Diego. ADNI data are disseminated by the Laboratory of Neuroimaging at the University of California, Los Angeles. This research was also supported by The American Heart Association and/or Bugher Foundation Centers for Stroke Prevention Research (grant number 0775010N); Deane Institute for Integrative Study of Atrial Fibrillation and Stroke; the National Center for Research Resources (grant number P41-RR14075); the National Institute for Biomedical Imaging and Bioengineering (grant number R01 EB006758); the National Institute on Aging (grant number AG02238); the National Institute of Health (R01AG031224 and T32 EB005970); and the National Institute for Neurological Disorders and Stroke (grant numbers R01 NS052585–01, R01 NS059727).

None of the sponsors had any role in design and conduct of the study, collection, or analysis of the data presented in this study. ADNI is sponsored by Pfizer Inc, Wyeth Research, Bristol-Myers Squibb, Eli Lilly, and Company, GlaxoSmithKline, Merck & Co Inc, AstraZeneca AB, Novartis Pharmaceuticals Corporation, Alzheimer's Association, Eisai Global Clinical Development, Elan Corporation plc, Forest Laboratories, and the Institute for the Study of Aging, with participation from the U.S. Food and Drug Administration. Dr Biffi received research support from The American Heart Association/Bugher Foundation Centers for Stroke Prevention Research (0775010N). Dr Desikan receives research support from the National Institute of Health (T32 EB005970 and R01AG031224). Dr Sabuncu received support from an NIH K25 grant (NIBIB 1K25EB013649-01) and a BrightFocus Foundation Alzheimer's research pilot grant (AHAF-A2012333). Mr Schmansky received research support from the National Center for Research Resources (P41-RR14075), the National Institute for Biomedical Imaging and Bioengineering (R01EB006758), the National Institute on Aging (AG02238), the National Institute for Neurological Disorders and Stroke (R01 NS052585-01), and The Autism and Dyslexia Project, funded by the Ellison Medical Foundation. Dr Salat is funded by NIH grant R01 NR010827, and receives research support from NIH grants R01-NS070963, R01-AG026484, R01-NS070834, P41-RR014075, R01-NS042861, R33-DA026104, as well as research support from VA Center of Excellence B6796-C and Biogen Idec. Dr Rosand is funded by NIH grants R01NS059727, U01NS069208, U01NS069763, R01NS063925, R01 HL093023. Dr Anderson is supported by a Clinical Research Training Fellowship from the American Brain Foundation, a Fellowship in Therapeutic Development from the Massachusetts General Hospital Department of Neurology in partnership with Biogen Idec, Inc, and a SPARK Award from the Massachusetts General Hospital Institute for Heart, Vascular, and Stroke Care. Alessandro Biffi, Christopher D. Anderson, and Jonathan Rosand contributed to the manuscript preperation. Alessandro Biffi and Christopher D. Anderson contributed to genetic data analysis. Rahul S. Desikan, Mert Sabuncu, Nick Schmansky, David Salat contributed to neuroimaging data analysis. David Salat, Jonathan Rosand, and Christopher D. Anderson contributed to study management. Alessandro Biffi, Christopher D. Anderson, Rahul S. Desikan, Mert Sabuncu, Nick Schmansky, David Salat, and Jonathan Rosand contributed to the manuscript review. All authors shared equal access to study data.

Appendix A. Supplementary data

Supplementary data associated with this article can be found, in the online version, at http://dx.doi.org/10.1016/j.neurobiolaging.2014.01.141.

References

Anderson, C.D., Biffi, A., Nalls, M.A., Devan, W.J., Schwab, K., Ayres, A.M., Valant, V., Ross, O.A., Rost, N.S., Saxena, R., Viswanathan, A., Worrall, B.B., Brott, T.G., Goldstein, J.N., Brown, D., Broderick, J.P., Norrving, B., Greenberg, S.M., Silliman, S.L., Hansen, B.M., Tirschwell, D.L., Lindgren, A., Slowik, A., Schmidt, R., Selim, M., Roquer, J., Montaner, J., Singleton, A.B., Kidwell, C.S., Woo, D., Furie, K.L., Meschia, J.F., Rosand, J., International Stroke Genetics Consortium, 2013. Common variants within oxidative phosphorylation genes influence risk of ischemic stroke and intracerebral hemorrhage. Stroke 44, 612–619.

Banerjee, S., 2012. The macroeconomics of dementia–will the world economy get Alzheimer's disease? Arch. Med. Res. 43, 705–709.

Beal, M.F., 1995. Aging, energy, and oxidative stress in neurodegenerative diseases. Ann. Neurol. 38, 357–366.

Bettens, K., Sleegers, K., Van Broeckhoven, C., 2013. Genetic insights in Alzheimer's disease. Lancet Neurol. 12, 92–104.

Biffi, A., Anderson, C.D., Desikan, R.S., Sabuncu, M., Cortellini, L., Schmansky, N., Salat, D., Rosand, J., Alzheimer's Disease Neuroimaging Initiative (ADNI), 2010a. Genetic variation and neuroimaging measures in Alzheimer disease. Arch. Neurol. 67, 677–685.

Biffi, A., Anderson, C.D., Nalls, M.A., Rahman, R., Sonni, A., Cortellini, L., Rost, N.S., Matarin, M., Hernandez, D.G., Plourde, A., de Bakker, P.I., Ross, O.A., Greenberg, S.M., Furie, K.L., Meschia, J.F., Singleton, A.B., Saxena, R., Rosand, J., 2010b. Principal-component analysis for assessment of population stratification in mitochondrial medical genetics. Am. J. Hum. Genet. 86, 904–917.

Chen, S.D., Chang, A.Y., Chuang, Y.C., 2010. The potential role of mitochondrial dysfunction in seizure-associated cell death in the hippocampus and epileptogenesis. J. Bioenerg. Biomembr. 42, 461–465.

de la Torre, J.C., 2008. Pathophysiology of neuronal energy crisis in Alzheimer's disease. Neurodegener. Dis. 5, 126–132.

Desikan, R.S., Cabral, H.J., Fischl, B., Guttmann, C.R., Blacker, D., Hyman, B.T., Albert, M.S., Killiany, R.J., 2009. Temporoparietal MR imaging measures of atrophy in subjects with mild cognitive impairment that predict subsequent diagnosis of Alzheimer disease. AJNR Am. J. Neuroradiol. 30, 532–538.

Dubois, B., Feldman, H.H., Jacova, C., Cummings, J.L., Dekosky, S.T., Barberger-Gateau, P., Delacourte, A., Frisoni, G., Fox, N.C., Galasko, D., Gauthier, S., Hampel, H., Jicha, G.A., Meguro, K., O'Brien, J., Pasquier, F., Robert, P., Rossor, M., Salloway, S., Sarazin, M., de Souza, L.C., Stern, Y., Visser, P.J., Scheltens, P., 2010. Revising the definition of Alzheimer's disease: a new lexicon. Lancet Neurol. 9, 1118–1127.

Eckert, A., Schulz, K.L., Rhein, V., Götz, J., 2010. Convergence of amyloid-beta and tau pathologies on mitochondria in vivo. Mol. Neurobiol. 41, 107–114.

Hochberg, Y., Benjamini, Y., 1990. More powerful procedures for multiple significance testing. Stat. Med. 9, 811–818.

Horan, M.P., Pichaud, N., Ballard, J.W., 2012. Review: quantifying mitochondrial dysfunction in complex diseases of aging. J. Gerontol. A Biol. Sci. Med. Sci. 67, 1022–1035.

Kalaria, R.N., 2002. Small vessel disease and Alzheimer's dementia: pathological considerations. Cerebrovasc. Dis. 13, 48–52.

Kalaria, R.N., Akinyemi, R., Ihara, M., 2012. Does vascular pathology contribute to Alzheimer changes? J. Neurol. Sci. 322, 141–147.

Killiany, R.J., Gomez-Isla, T., Moss, M., Kikinis, R., Sandor, T., Jolesz, F., Tanzi, R., Jones, K., Hyman, B.T., Albert, M.S., 2000. Use of structural magnetic resonance imaging to predict who will get Alzheimer's disease. Ann. Neurol. 47, 430–439.

Morán, M., Moreno-Lastres, D., Marín-Buera, L., Arenas, J., Martín, M.A., Ugalde, C., 2012. Mitochondrial respiratory chain dysfunction: implications in neurodegeneration. Free Radic. Biol. Med. 53, 595–609.

Petersen, R.C., Aisen, P.S., Beckett, L.A., Donohue, M.C., Gamst, A.C., Harvey, D.J., Jack Jr., C.R., Jagust, W.J., Shaw, L.M., Toga, A.W., Trojanowski, J.Q., Weiner, M.W., 2010. Alzheimer's disease neuroimaging initiative (ADNI): clinical characterization. Neurology 74, 201–209.

Rhein, V., Song, X., Wiesner, A., Ittner, L.M., Baysang, G., Meier, F., Ozmen, L., Bluethmann, H., Dröse, S., Brandt, U., Savaskan, E., Czech, C., Götz, J., Eckert, A., 2009. Amyloid-beta and tau synergistically impair the oxidative phosphorylation system in triple transgenic Alzheimer's disease mice. Proc. Natl. Acad. Sci. U.S.A 106, 20057–20062.

Schmitt, K., Grimm, A., Kazmierczak, A., Strosznajder, J.B., Götz, J., Eckert, A., 2012. Insights into mitochondrial dysfunction: aging, amyloid-β, and tau-A deleterious trio. Antioxid. Redox Signal. 16, 1456–1466.

Shaw, L.M., Vanderstichele, H., Knapik-Czajka, M., Clark, C.M., Aisen, P.S., Petersen, R.C., Blennow, K., Soares, H., Simon, A., Lewczuk, P., Dean, R., Siemers, E., Potter, W., Lee, V.M., Trojanowski, J.Q., Alzheimer's Disease Neuroimaging Initiative, 2009. Cerebrospinal fluid biomarker signature in Alzheimer's disease neuroimaging initiative subjects. Ann. Neurol. 65, 403–413.

Snowdon, D.A., Greiner, L.H., Mortimer, J.A., Riley, K.P., Greiner, P.A., Markesbery, W.R., 1997. Brain infarction and the clinical expression of Alzheimer disease. The Nun Study. JAMA 277, 813–817.

Sosa-Ortiz, A.L., Acosta-Castillo, I., Prince, M.J., 2012. Epidemiology of dementias and Alzheimer's disease. Arch. Med. Res. 43, 600–608.

Stefanatos, R., Sanz, A., 2011. Mitochondrial complex I: a central regulator of the aging process. Cell Cycle 10, 1528–1532.

Subramanian, A., Tamayo, P., Mootha, V.K., Mukherjee, S., Ebert, B.L., Gillette, M.A., Paulovich, A., Pomeroy, S.L., Golub, T.R., Lander, E.S., Mesirov, J.P., 2005. Gene set enrichment analysis: a knowledge-based approach for interpreting genome-wide expression profiles. Proc. Natl. Acad. Sci. U.S.A 102, 15545–15550.

Thal, D.R., Ghebremedhin, E., Orantes, M., Wiestler, O.D., 2003. Vascular pathology in Alzheimer disease: correlation of cerebral amyloid angiopathy and arteriosclerosis/lipohyalinosis with cognitive decline. J. Neuropathol. Exp. Neurol. 62, 1287–1301.

Verri, M., Pastoris, O., Dossena, M., Aquilani, R., Guerriero, F., Cuzzoni, G., Venturini, L., Ricevuti, G., Bongiorno, A.I., 2012. Mitochondrial alterations, oxidative stress and neuroinflammation in Alzheimer's disease. Int. J. Immunopathol. Pharmacol. 25, 345–353.

Wagner, B.K., Kitami, T., Gilbert, T.J., Peck, D., Ramanathan, A., Schreiber, S.L., Golub, T.R., Mootha, V.K., 2008. Large-scale chemical dissection of mitochondrial function. Nat. Biotechnol. 26, 343–351.

Wang, K., Li, M., Bucan, M., 2007. Pathway-based approaches for analysis of genomewide association studies. Am. J. Hum. Genet. 81, 1278–1283.

Weiner, M.W., Veitch, D.P., Aisen, P.S., Beckett, L.A., Cairns, N.J., Green, R.C., Harvey, D., Jack, C.R., Jagust, W., Liu, E., Morris, J.C., Petersen, R.C., Saykin, A.J., Schmidt, M.E., Shaw, L., Siuciak, J.A., Soares, H., Toga, A.W., Trojanowski, J.Q., Alzheimer's Disease Neuroimaging Initiative, 2012. The Alzheimer's disease neuroimaging initiative: a review of papers published since its inception. Alzheimers Dement. 8, S1–S68.